Journal of Nuclear Materials 305 (2002) 83–89

journal of nuclear materials

www.elsevier.com/locate/jnucmat

Sub-solidus phase equilibria in the CeO_2–ThO_2–ZrO_2 system

V. Grover, A.K. Tyagi *

Applied Chemistry Division, Bhabha Atomic Research Centre, Trombay, Mumbai 400 085, India

Received 24 April 2002; accepted 3 August 2002

Abstract

The phase relations in the CeO_2–ThO_2–ZrO_2 system have been established after slowly cooling the samples from 1400 °C. Ceria has been used as a surrogate material in place of plutonia. The various phase boundaries were delineated by refining the powder XRD data. Thoria and ceria were shown to form an ideal solid solution in the complete homogeneity range. About 5 and 20 mol.% of zirconia can be dissolved, under the heating conditions used in the present investigations, in the lattice of thoria and ceria, respectively. In the ZrO_2–$Th_{0.5}Ce_{0.5}O_2$ system, 10 mol.% zirconia was found to get incorporated in the lattice of $Th_{0.5}Ce_{0.5}O_2$. The $(Th_{0.5}Zr_{0.5})_{1-x}Ce_xO_2$ system shows the formation of single-phase solid solutions from $x \geqslant 0.70$. Thorium rich compositions in $(Ce_{0.5}Zr_{0.5})_{1-x}Th_xO_2$ system were also found to be cubic solid solution. In addition, a number of other phases like t-ZrO_2, various two-phase and multi-phase regions could also be identified in this pseudo-ternary system.

1. Introduction

The development of uranium free inert matrix fuel is of world-wide interest as by using this concept it is possible to faster annihilate the large stock of plutonium available from the dismantled weapons and the accumulated stock from the nuclear power plants. In order to develop new inert matrix fuel host lattices several groups all over the world are engaged in research [1–5]. Kleykamp [6] has written a lucid review on the selection of materials as diluents for burning the plutonium. In addition, this concept is also being contemplated to prepare targets for minor actinides transmutation. In these fuels, an inert matrix serves as a support for the actinide phases, as does the non-fissile $^{238}UO_2$ matrix for PuO_2 in a typical fast breeder MOX fuel. However, ^{238}U is fertile and is a source of formation of additional plutonium and other transuranium elements, which are undesirable from the point of view of non-proliferation. The inert matrix, as suggested by its name, does not lead to the formation of any fissile material, after the irradiation. A material to act as an inert matrix has to satisfy a number of stringent conditions e.g., a good neutron economy, superior thermophysical properties (high thermal conductivity, low thermal expansion etc.), absence of phase changes and decomposition at higher temperature, compatibility with the cladding material, stability against radiation, good mechanical properties, insignificant leachability and low cost. A number of host lattices are being considered to act as an inert matrix, for diluting plutonium, viz., multi-phase ceramic–ceramic composites based on zirconia, alumina or magnesia, $Al_5Y_3O_{12}$, MgO, $MgAl_2O_4$, ROX (rock-like oxides) [7]. Several ceramic composites like yttria-stabilized zirconia (YSZ)–Al_2O_3–$MgAl_2O_4$, YSZ–$MgAl_2O_4$, ThO_2–$MgAl_2O_4$, etc. have also been proposed. Several nitrides, carbides [5] and phosphates [8] are also being contemplated to act as an inert matrix.

India has very large deposits of thorium, which are envisaged to be used for nuclear power production. Thoria being a very stable oxide (chemically inert), could also be considered as a potential host for diluting and burning plutonia, though it is not exactly an inert matrix

---

* Corresponding author. Tel.: +91-22 559 5330; fax: +91-22 550 5151.

E-mail address: aktyagi@magnum.barc.ernet.in (A.K. Tyagi).

0022-3115/02/$ - see front matter © 2002 Elsevier Science B.V. All rights reserved.
PII: S0022-3115(02)01157-1

in a conventional sense. India has a long-term program on thoria utilization. In this context, it is considered worthwhile to investigate inert matrices coupled with thoria for plutonia burning. In addition, inclusion of thoria is likely to improve the neutron economy and in situ produced U-233 would increase the burn-up of the inert matrix based fuel [9].

Therefore, the CeO_2–ThO_2–ZrO_2 system has a relevance to the inert matrix project. Ceria is used as a surrogate material [10,11] in place of plutonia. There are several reports on pseudo-binary phase diagrams/phase relations in systems like ThO_2–CeO_2 [11], CeO_2–ZrO_2 [12] and ThO_2–ZrO_2 [13]. Whitfield et al. [14] reported X-ray studies of the mixed oxides in the ThO_2–CeO_2–Ce_2O_3 system. Thoria and ceria were shown to form an ideal solid solution in the complete homogeneity range [11]. The phase relations in the ThO_2–ZrO_2 system [13], under melt and quenching (from 3000 °C) conditions, showed the solubility of zirconia in the thoria lattice over a wide homogeneity range, while retaining the fluorite structure. Later it was reported by Brisi [15] that about 5 mol.% ZrO_2 can be retained in the lattice of thoria even at about 1000 °C. The phase diagram of the CeO_2–ZrO_2 system consists of two regions namely a monoclinic solid solution up to about 18 mol.% ceria into zirconia and a two-phase region consisting of a tetragonal and a cubic solid solution. On heating to appropriately higher temperatures, depending upon the composition, the monoclinic and tetragonal solid solutions were shown to become tetragonal and cubic solid solutions, respectively. In order to identify still newer inert matrices, it is required to construct the sub-solidus phase equilibria in the desired system so as to identify suitable single-phase compositions. It may be added here that the pseudo-ternary phase diagrams on nuclear materials are not well reported compared to the pseudo-binary phase diagrams. Schleifer et al. [16] reported phase equilibria in the UO_2–ZrO_2–Ln_2O_3 (Ln = Lanthanides) system in the temperature range 1270–1670 K. The samples were prepared by a hydrolysis method in their study. In this manuscript, the sub-solidus phase equilibria in the CeO_2–ThO_2–ZrO_2 system under slow cooled conditions is being reported.

2. Experimental

CeO_2, ZrO_2 and ThO_2 (all 99.9%) were used as the starting materials, which were heated at 900 °C for overnight prior to the further use. These starting materials were well characterized by powder XRD before use. About 80 compositions in the CeO_2–ThO_2–ZrO_2 system were prepared by a three-stage heating protocol, as follows: the intimately ground mixtures were heated in the pellet form at 1200 °C for 36 h, followed by second heating at 1300 °C for 36 h after regrinding and repelletising. In order to attain a better homogeneity, the products obtained after second heating were again reground, pelletised and heated at 1400 °C for 48 h, which was the final annealing temperature of all the specimens. The heating and cooling rates were $2° \text{ min}^{-1}$ in all the annealing steps and the atmosphere was static air. The XRD patterns were recorded on a Philips X-ray diffractometer (Model PW 1710) with monochromatized CuKα radiation ($K\alpha_1 = 154.06$ pm and $K\alpha_2 = 154.44$ pm). Silicon was used as an external standard for calibration of the instrument. The XRD patterns were well analyzed by comparing with the reported ones. In order to determine the solubility limits, the lattice parameters were refined by a least-squares method.

3. Results and discussion

The ThO_2–CeO_2 system showed the formation of a solid solution in the complete homogeneity range under the present experimental conditions. This observation is in agreement with our earlier results [10]. The variation of the lattice parameter as a function of the ceria content in $Th_{1-x}Ce_xO_2$ $(0.0 \leqslant x \leqslant 1.0)$ solid solution is represented as follows:

$$\text{Lattice parameter of } Th_{1-x}Ce_xO_2\, a = 0.5597 - 0.0187x \text{ (nm)}. \tag{1}$$

The XRD patterns of the various products in $Th_{1-x}Zr_xO_2$ system were refined and the lattice parameters are compiled in Table 1. However, the XRD pattern of the minor products in the mixtures could not be refined due the presence of only a few lines. The volume of the $Th_{0.95}Zr_{0.05}O_2$ lattice was found to be as 0.1744(1) nm^3 as compared to 0.1756(1) nm^3 for pure thoria. The lattice parameter did not decrease in subsequent compositions towards the ZrO_2 side (Fig. 1), thereby indicating that only about 5 mol.% of zirconia can be dissolved in the lattice of ThO_2, which is in good agreement with the reported solubility limit [15] under quenched conditions. The XRD pattern of the subsequent compositions towards the ZrO_2 end revealed the appearance of monoclinic zirconia peaks. The unit cell volume of pure zirconia was 0.1407(1) nm^3, which did not increase even at the nominal composition $Th_{0.05}Zr_{0.95}O_2$ indicating that thoria has virtually no solubility in zirconia under the heat treatment used in the present study. Thus there is a phase separation from the nominal composition $Th_{0.95}Zr_{0.05}O_2$ to $Th_{0.05}Zr_{0.95}O_2$ in the ThO_2–ZrO_2 system. It may be noted that the phase diagram of the ThO_2–ZrO_2 system, as reported by Duwez and Loh [13] shows a phase separation throughout the range in the low temperature region of the ThO_2–ZrO_2 phase diagram. Probably, they did not

Table 1
Phase analysis and room temperature lattice parameters of the phases in $Th_{1-x}Zr_xO_2$ system, annealed at 1400 °C (in air) followed by slow cooling

S. no.	Nominal composition	Phase analysis	a (nm)	b (nm)	c (nm)	β (°)	Volume (nm^3)
1	ThO_2	C	0.5600(1)				0.1756(1)
2	$Th_{0.95}Zr_{0.05}O_2$	C	0.5587(1)				0.1744(1)
3	$Th_{0.92}Zr_{0.08}O_2$	C	0.5590(1)				0.1746(1)
4	$Th_{0.90}Zr_{0.10}O_2$	C	0.5587(1)				0.1744(1)
		M	–[a]				
5	$Th_{0.80}Zr_{0.20}O_2$	C	0.5586(2)				0.1743(9)
		M	–[a]				
6	$Th_{0.70}Zr_{0.30}O_2$	C	0.5588(1)				0.1745(1)
		M	–[a]				
7	$Th_{0.60}Zr_{0.40}O_2$	C	0.5594(3)				0.1750(1)
		M	–[a]				
8	$Th_{0.50}Zr_{0.50}O_2$	C	0.5593(1)				0.1749(1)
		M	–[a]				
9	$Th_{0.40}Zr_{0.60}O_2$	C	0.5592(1)				0.1748(1)
		M	0.5307(6)	0.5209(7)	0.5155(3)	99.05(9)	0.1407(3)
10	$Th_{0.30}Zr_{0.70}O_2$	C	0.5589(1)				0.1746(1)
		M	–[a]				
11	$Th_{0.20}Zr_{0.80}O_2$	C	0.5588(1)				0.1745(1)
		M	0.5311(3)	0.5205(2)	0.5154(2)	99.13(5)	0.1407(1)
12	$Th_{0.10}Zr_{0.90}O_2$	C	0.5586(2)				0.1743(1)
		M	0.5311(3)	0.5207(2)	0.5147(2)	99.07(5)	0.1406(1)
13	$Th_{0.08}Zr_{0.92}O_2$	C	0.5588(1)				0.1745(1)
		M	0.5318(2)	0.5213(2)	0.5154(2)	99.20(4)	0.1410(1)
14	$Th_{0.05}Zr_{0.95}O_2$	C	0.5588(1)				0.1744(1)
		M	0.5314(3)	0.5210(2)	0.5147(2)	99.15(5)	0.1407(1)
15	ZrO_2	M	0.5313(1)	0.5212(1)	0.5147(1)	99.22(1)	0.1407(1)

C: cubic solid solution; M: monoclinic zirconia.

[a] Not refined due to insignificant intensity.

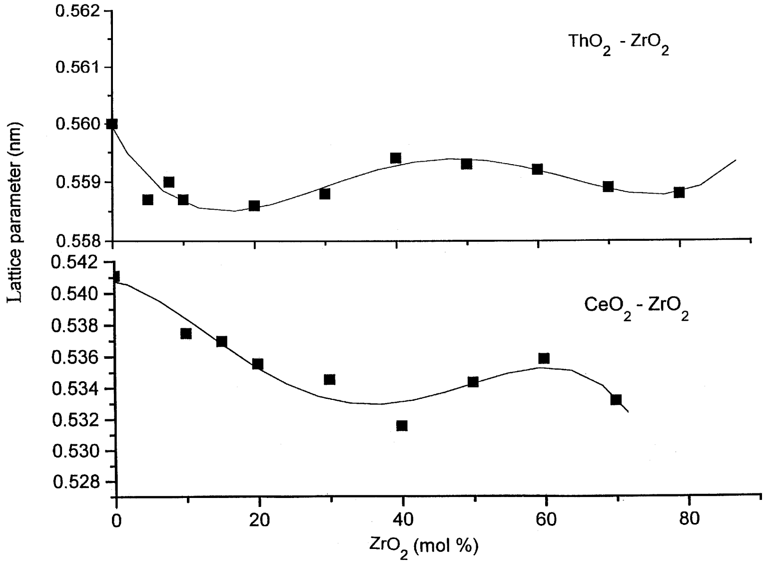

Fig. 1. Variation of the lattice parameter of the cubic phases in the ThO_2–ZrO_2 and CeO_2–ZrO_2 systems as a function of zirconia content.

Table 2
Phase analysis and room temperature lattice parameters of the phases in $Ce_{1-x}Zr_xO_2$ system, annealed at 1400 °C (in air) followed by slow cooling

S. no.	Nominal composition	Phase analysis	*a* (nm)	*b* (nm)	*c* (nm)	*β* (°)	Volume (nm^3)
1	CeO_2	C	0.5411(1)				0.1584(1)
2	$Ce_{0.90}Zr_{0.10}O_2$	C	0.5375(1)				0.1553(1)
3	$Ce_{0.85}Zr_{0.15}O_2$	C	0.5370(1)				0.1549(1)
4	$Ce_{0.80}Zr_{0.20}O_2$	C	0.5356(1)				0.1536(1)
5	$Ce_{0.70}Zr_{0.30}O_2$	C	0.5346(1)				0.1528(1)
		T	–[a]				
6	$Ce_{0.60}Zr_{0.40}O_2$	C	0.5316(1)				0.1503(1)
		T	–[a]				
7	$Ce_{0.50}Zr_{0.50}O_2$	C	0.5344(1)				0.1526(1)
		T	0.5141(5)		0.5254(8)		0.1388(3)
8	$Ce_{0.40}Zr_{0.60}O_2$	C	0.5359(3)				0.1539(1)
		T	0.5145(9)		0.526(1)		0.1394(5)
9	$Ce_{0.30}Zr_{0.70}O_2$	C	0.5332(4)				0.1516(2)
		T	0.5126(6)		0.5242(10)		0.1377(4)
10	$Ce_{0.20}Zr_{0.80}O_2$	T	0.5140(5)		0.5224(6)		0.1380(2)
		M	–[a]				
11	$Ce_{0.10}Zr_{0.90}O_2$	T	–[a]				
		M					
12	$Ce_{0.05}Zr_{0.95}O_2$	T	–[a]				
		M	0.5346(2)	0.5218(1)	0.5174(1)	99.05(3)	0.1425(1)
13	ZrO_2	M	0.5313(1)	0.5212(1)	0.5147(1)	99.22(1)	0.1407(1)

C: cubic solid solution; T: tetragonal zirconia; M: monoclinic zirconia.

[a] Not refined due to insignificant intensity.

investigate the composition $Th_{0.95}Zr_{0.05}O_2$ and directly went to the $Th_{0.90}Zr_{0.10}O_2$ composition.

Based on the lattice parameters (Table 2) in the $Ce_{1-x}Zr_xO_2$ series ($0.0 \leqslant x \leqslant 1.0$), it can be inferred that about 20 mol.% ZrO_2 is soluble in the lattice of ceria while maintaining single-phase. The lattice parameter of the cubic phase further decreases up to the composition $Ce_{0.60}Zr_{0.40}O_2$ (Fig. 1), but an additional phase also appears in compositions beyond $Ce_{0.80}Zr_{0.20}O_2$. This observation indicates that the solubility of zirconia in ceria is slightly higher than 20 mol.% but probably one has to quench the samples so as to avoid the phase separation which might have occurred during slow cooling. A nearly single-phase tetragonal zirconia-type modification was obtained at the nominal composition $Ce_{0.20}Zr_{0.80}O_2$, which is in reasonably good agreement with an earlier report [17] in which a single-phase tetragonal zirconia was obtained at the nominal composition $Ce_{0.16}Zr_{0.84}O_2$. An important observation of this system is the absence of the cubic zirconia phase. Thus probably instead of isovalent substitution, one needs substitution by a suitable aliovalent ion, ca. Y^{3+} or Ca^{2+} or Ce^{3+}, e.g., $Zr_{1-x}Ce_xO_{2-y}$ with oxygen vacancies, to stabilize the cubic zirconia. Stoichiometric cubic $Zr_{1-x}Ce_xO_2$, i.e., without oxygen vacancies, is reported [13] to be formed at very high temperatures (above 2000 °C).

In pseudo-ternary systems, ZrO_2–$Th_{0.5}Ce_{0.5}O_2$, CeO_2–$Th_{0.5}Zr_{0.5}O_2$ and ThO_2–$Zr_{0.5}Ce_{0.5}O_2$ were chosen as the end members (Fig. 2), i.e., the compositions corresponding to the center of the sides of an equilateral

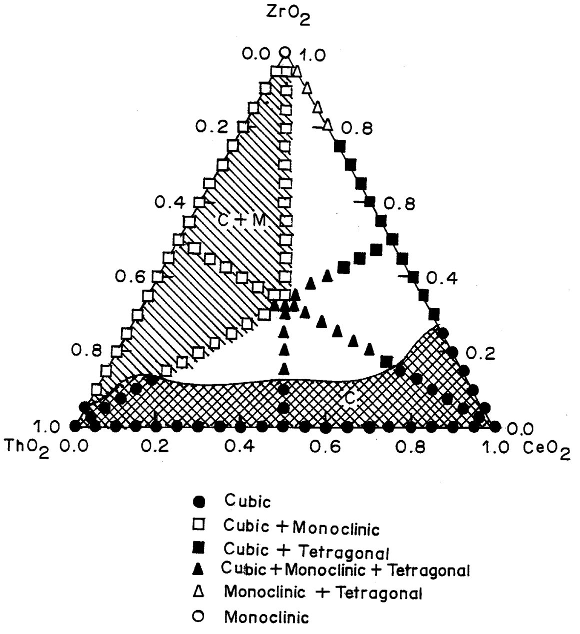

Fig. 2. Phase relations in the pseudo-ternary CeO_2–ThO_2–ZrO_2 system.

triangle and the corresponding opposite apex. As it is seen while investigating binary systems that among these three chosen binary end members only $Th_{0.5}Ce_{0.5}O_2$ is a single-phase material. The results of the phase analysis of each ternary series are as follows.

Only 10 mol.% zirconia in the ZrO_2–$Th_{0.5}Ce_{0.5}O_2$ system was found to get incorporated in the lattice of $Th_{0.5}Ce_{0.5}O_2$. A phase separation into the cubic thoria–ceria solid solution, t-ZrO_2 and m-ZrO_2 was observed from the nominal composition $Th_{0.425}Ce_{0.425}Zr_{0.15}O_2$ to $Th_{0.35}Ce_{0.35}Zr_{0.30}O_2$. The amount of t-$ZrO_2$ is insignificant as only its 100% peak at $2\theta \approx 30°$ is present throughout in this range. The t-ZrO_2 phase disappeared completely from the composition $Th_{0.05}Ce_{0.05}Zr_{0.90}O_2$ onwards i.e., in zirconia rich compositions. The intensity of the cubic solid solution was insignificant in the composition $Th_{0.025}Ce_{0.025}Zr_{0.95}O_2$. It appears, based on the slight increase in lattice parameter of m-ZrO_2 (Table 3), that this nominal composition is a two-phase mixture of a solid solution (2.5 mol.% CeO_2 in zirconia) and ThO_2.

The nominal composition of the end member of the CeO_2–$Th_{0.5}Zr_{0.5}O_2$ system is $Th_{0.5}Zr_{0.5}O_2$, which itself is a two-phase mixture, consisting of a cubic solid solution and m-ZrO_2. The phase analysis of $(Th_{0.5}Zr_{0.5})_{1-x}Ce_xO_2$ revealed a two-phase region, consisting of the cubic solid solution and m-ZrO_2 up $x = 0.30$. The lattice parameter of the cubic solid solution decreases in the series, indicating that ceria is getting incorporated in the lattice of thoria. The lattice parameters of m-ZrO_2 could not be refined as only a few peaks were observed, probably due to a poor X-ray scattering power of Zr compared to that of Th. The compositions higher than $x = 0.3$ were found to have a small amount of t-ZrO_2 also. The m-ZrO_2 phase disappeared at the composition $Th_{0.175}Zr_{0.175}Ce_{0.65}O_2$. The single-phase cubic solid solution was observed in this series from $x = 0.70$ to 1.0. The lattice parameter of ceria is 0.5411(1) nm, which decreases systematically up to $x = 0.75$ but surprisingly it increases in the composition $Th_{0.15}Zr_{0.15}Ce_{0.70}O_2$ and in the cubic compositions thereafter (i.e., $x = 0.70$). This change over in the trend of the lattice parameter variation is attributed to the opposite effects of the incorporation of Th^{4+} and Zr^{4+} into the lattice of CeO_2 due to relative ionic size considerations (Table 4).

The nominal composition of the end member of the third pseudo-ternary system ThO_2–$Zr_{0.5}Ce_{0.5}O_2$ is $Ce_{0.5}Zr_{0.5}O_2$, which itself is a two-phase mixture, consisting of

Table 3
Phase analysis and room temperature lattice parameters of the phases in $(Th_{0.5}Ce_{0.5})_{1-x}Zr_xO_2$ system, annealed at 1400 °C (in air) followed by slow cooling

S. no.	Nominal composition	Phase analysis	*a* (nm)	*b* (nm)	*c* (nm)	*β* (°)	Volume (nm³)
1	$Th_{0.5}Ce_{0.5}Zr_{0.00}O_2$	C	0.5496(1)				0.1660(1)
2	$Th_{0.45}Ce_{0.45}Zr_{0.10}O_2$	C	0.5487(1)				0.1652(1)
3	$Th_{0.425}Ce_{0.425}Zr_{0.15}O_2$	C	0.5487(1)				0.1652(1)
		T	–[a]				
		M	–[a]				
4	$Th_{0.40}Ce_{0.40}Zr_{0.20}O_2$	C	0.5487(1)				0.1648(1)
		T	–[a]				
		M	–[a]				
5	$Th_{0.35}Ce_{0.35}Zr_{0.30}O_2$	C	0.5482(1)				0.1652(1)
		T	–[a]				
		M	–[a]				
6	$Th_{0.30}Ce_{0.30}Zr_{0.40}O_2$	C	0.5487(1)				0.1655(1)
		M	–[a]				
7	$Th_{0.25}Ce_{0.25}Zr_{0.50}O_2$	C	0.5490(1)				0.1658(1)
		M	–[a]				
8	$Th_{0.20}Ce_{0.20}Zr_{0.60}O_2$	C	0.5494(1)				0.1662(1)
		M	0.532(1)	0.5197(9)	0.517(1)	98.6(2)	0.1416(6)
9	$Th_{0.15}Ce_{0.15}Zr_{0.70}O_2$	C	0.5499(1)				0.1662(1)
		M	0.5338(5)	0.5210(5)	0.5168(5)	98.89(8)	0.1420(2)
10	$Th_{0.10}Ce_{0.10}Zr_{0.80}O_2$	C	0.5493(2)				0.1657(1)
		M	0.5346(6)	0.5222(6)	0.5180(6)	99.03(9)	0.1428(3)
11	$Th_{0.05}Ce_{0.05}Zr_{0.90}O_2$	C	0.5530(2)				0.1692(1)
		M	0.5332(4)	0.5216(3)	0.5166(4)	98.97(6)	0.1419(2)
12	$Th_{0.025}Ce_{0.025}Zr_{0.95}O_2$	C	–[a]				
		M	0.5336(5)	0.5217(3)	0.5164(4)	99.04(6)	0.1420(2)
13	ZrO_2	M	0.5313(1)	0.5212(1)	0.5147(1)	99.22(1)	0.1407(1)

[a] Not refined due to insignificant intensity.

Table 4
Phase analysis and room temperature lattice parameters of the products in $(Th_{0.5}Zr_{0.5})_{1-x}Ce_xO_2$ system, annealed at 1400 °C (in air) followed by slow cooling

S. no.	Nominal composition	Phase analysis	*a* (nm)	Volume (nm^3)
1	$Th_{0.5}Zr_{0.5}Ce_{0.00}O_2$	C	0.5593(1)	0.1749(1)
		M	–[a]	
2	$Th_{0.45}Zr_{0.45}Ce_{0.10}O_2$	C	0.5555(1)	0.1714(1)
		M	–[a]	
3	$Th_{0.40}Zr_{0.40}Ce_{0.20}O_2$	C	0.5531(1)	0.1692(1)
		M	–[a]	
4	$Th_{0.35}Zr_{0.35}Ce_{0.30}O_2$	C	0.549(1)	0.1658(1)
		M		
5	$Th_{0.30}Zr_{0.30}Ce_{0.40}O_2$	C	0.5470(1)	0.1637(1)
		T	–[a]	
		M	–[a]	
6	$Th_{0.25}Zr_{0.25}Ce_{0.50}O_2$	C	0.5448(1)	0.1617(1)
		T	–[a]	
		M	–[a]	
7	$Th_{0.20}Zr_{0.20}Ce_{0.60}O_2$	C	0.5425(1)	0.1597(1)
		T	–[a]	
		M	–[a]	
9	$Th_{0.175}Zr_{0.175}Ce_{0.65}O_2$	C	0.5411(1)	0.1585(1)
		T	–[a]	
10	$Th_{0.15}Zr_{0.15}Ce_{0.70}O_2$	C	0.5407(1)	0.1581(1)
11	$Th_{0.125}Zr_{0.125}Ce_{0.75}O_2$	C	0.5397(1)	0.1572(1)
12	$Th_{0.10}Zr_{0.10}Ce_{0.80}O_2$	C	0.5404(1)	0.1578(1)
13	$Th_{0.05}Zr_{0.05}Ce_{0.90}O_2$	C	0.5409(1)	0.1582(1)
14	CeO_2	C	0.5411(1)	0.1584(1)

[a] Not refined due to insignificant intensity.

Table 5
Phase analysis and room temperature lattice parameters of the products in $(Ce_{0.5}Zr_{0.5})_{1-x}Th_xO_2$ system, annealed at 1400 °C (in air) followed by slow cooling

S. no.	Nominal composition	Phase analysis	*a* (nm)	Volume (nm^3)
1	$Ce_{0.5}Zr_{0.5}Th_{0.00}O_2$	C	0.5344(1)	0.1526(1)
		T, *a*	0.5141(5)	0.1388(3)
		T, *c*	0.5254(8)	
2	$Ce_{0.45}Zr_{0.45}Th_{0.10}O_2$	C	0.5404(1)	0.1578(1)
		T	–[a]	
3	$Ce_{0.40}Zr_{0.40}Th_{0.20}O_2$	C	0.5449(1)	0.1618(1)
		T	–[a]	
		M	–[a]	
4	$Ce_{0.35}Zr_{0.35}Th_{0.30}O_2$	C	0.5481(1)	0.1646(1)
		T	–[a]	
		M	–[a]	
5	$Ce_{0.30}Zr_{0.30}Th_{0.40}O_2$	C	0.5507(1)	0.1670(1)
		M	–[a]	
6	$Ce_{0.25}Zr_{0.25}Th_{0.50}O_2$	C	0.5527(1)	0.1688(1)
		M	–[a]	
7	$Ce_{0.20}Zr_{0.20}Th_{0.60}O_2$	C	0.5545(1)	0.1705(1)
		M	–[a]	
8	$Ce_{0.15}Zr_{0.15}Th_{0.70}O_2$	C	0.5559(1)	0.1718(1)
		M	–[a]	
9	$Ce_{0.125}Zr_{0.125}Th_{0.75}O_2$	C	0.5568(1)	0.1726(1)
10	$Ce_{0.10}Zr_{0.10}Th_{0.80}O_2$	C	0.5570(1)	0.1728(1)
11	$Ce_{0.05}Zr_{0.05}Th_{0.90}O_2$	C	0.5579(1)	0.1737(1)
12	ThO_2	C	0.5600(1)	0.1756(1)

[a] Not refined due to insignificant intensity.

a cubic solid solution and t-ZrO_2. The m-ZrO_2 phase appears at $Ce_{0.40}Zr_{0.40}Th_{0.20}O_2$, which persists up to the composition $Ce_{0.15}Zr_{0.15}Th_{0.70}O_2$. The compositions $Ce_{0.125}Zr_{0.125}Th_{0.75}O_2$ onwards exist as a single cubic phase. The lattice parameter also systematically varies (Table 5).

4. Conclusions

The detailed phase relation studies in the pseudo-ternary system CeO_2–ZrO_2–ThO_2 revealed several interesting features. Based on the refinement of the XRD data, several phase regions namely, cubic solid solutions, two-phase and multi-phase regions could be delineated. Ceria and thoria have appreciable solubilities of nominal compositions $Th_{0.5}Zr_{0.5}O_2$ and $Ce_{0.5}Zr_{0.5}O_2$, respectively, whereas the ZrO_2 lattice does not accommodate any $Ce_{0.5}Th_{0.5}O_2$. A cubic solid solution phase field and a two-phase field (cubic + monoclinic) could be delineated unequivocally. To our best knowledge this is the first detailed study of phase relations in the CeO_2–ThO_2–ZrO_2 system. The single-phase ternary compositions, as found in this study, are expected to be superior compared to the multi-phase compositions, for plutonium utilization. The phase equilibria in CeO_2–ThO_2–ZrO_2 can be used to simulate the phase equilibria in the PuO_2–ThO_2–ZrO_2 system. The corresponding phase equilibria in the CeO_2–ThO_2–ZrO_2 system under quenched conditions is being worked out.

Acknowledgements

The authors thank Dr N.M. Gupta, Head, Applied Chemistry Division, Bhabha Atomic Research Centre, for his keen interest and encouragement during the course of this work. Ms A.B. Sonawane is thanked for assistance during the course of this work.

References

[1] H. Akie, T. Muromura, H. Takano, S. Matsura, Nucl. Technol. 107 (1994) 182.
[2] J.M. Paratte, R. Chawla, Ann. Nucl. Energy 22 (1995) 471.
[3] C. Lombardi, A. Mazzola, Ann. Nucl. Energy 23 (1996) 1117.
[4] K. Ferguson, Trans. Am. Nucl. Soc. 75 (1996) 75.

[5] M. Burghartz, H. Matzke, C. Leger, G. Vambenepe, M. Rome, J. Alloys Compd. 271–273 (1998) 544.

[6] H. Kleykamp, J. Nucl. Mater. 275 (1999) 1.

[7] C. Degueldre, J.M. Paratte, J. Nucl. Mater. 274 (1999) 1.

[8] K. Bakker, H. Hein, R.J.M. Konings, R.R. van der Laan, H. Matzke, P. Van Vlaanderen, J. Nucl. Mater. 252 (1998) 228.

[9] F. Vettraino, G. Magnani, T. La Torretta, E. Marmo, S. Coelli, L. Luzzi, P. Ossi, G. Zappa, J. Nucl. Mater. 274 (1999) 23.

[10] M.D. Mathews, B.R. Ambekar, A.K. Tyagi, J. Nucl. Mater. 288 (2001) 83.

[11] A.K. Tyagi, B.R. Ambekar, M.D. Mathews, J. Alloys Compd. 337 (2002) 275.

[12] P. Duwez, F. Odell, J. Am. Ceram. Soc. 33 (1950) 280.

[13] P. Duwez, E. Loh, J. Am. Ceram. Soc. 40 (1957) 321.

[14] H.J. Whitfield, D. Roman, A.R. Palmer, J. Inorg. Nucl. Chem. 28 (1966) 2817.

[15] C. Brisi, Atti della Accademia delle Scienze di Torino 94 (1959) 67.

[16] F. Schleifer, A. Naoumidis, H. Nickel, J. Nucl. Mater. 101 (1981) 150.

[17] S. Meriani, G. Spinolo, Powder Diffr. 2 (1987) 255.